

Concentrated Polymer Solutions:

Part III. Normal Stresses in Simple Shear Flow

MICHAEL C. WILLIAMS

University of California, Berkeley, California

A molecular theory for the stress \mathbf{P} in a concentrated polymer solution is evaluated for simple shear flow. Three rheological functions (P_{12} , $P_{11} - P_{22}$, $P_{11} - P_{33}$) are predicted to be dependent on shear rate $\dot{\gamma}$ in a very complicated fashion, and are displayed graphically. A unique feature is that $P_{22} - P_{33}$ is shown to have the same sign as $P_{11} - P_{33}$ at low shear, a result in agreement with most experimental data and not predicted by other theories. A comparison with two sets of data verifies the prediction of relative behavior of shear and normal stresses at low $\dot{\gamma}$, but the theory fails to fit data at high $\dot{\gamma}$. Reasons for the success of the reducing factors c^2 or c^3 (where c is mass concentration) in constructing master curves for normal stress are suggested.

The shear-dependent stress properties of polymer solutions can be described by molecular theory only under very restricted circumstances. Only for the extremes of very concentrated rubbery liquids (3, 15, 28) and certain very dilute solutions (21, 29) have results been even moderately successful. In a preceding paper (26) we attempted to show how solutions of intermediate* concentration might be treated. The influence of intermolecular forces was explicitly considered, and a non-Newtonian viscosity was calculated for one simple model. As a further illustration, and to explore a more subtle nonlinear phenomenon, we shall here investigate the normal stress predictions for the same model.

THEORY

Here we shall summarize the theory which has been given previously in more detail (26). Linear polymer molecules, present in a solution of concentration n , are idealized as pearl necklace chains of N segments. Each segment in solution interacts with the solvent through a friction constant, and with other segments through a force potential U which depends on all the $3(nN)$ segment coordinates. Fixman has shown that, with certain restrictions (6, 26), the total stress tensor \mathbf{P} for such a solution may be represented by

$$\mathbf{P} = \mathbf{P}_0 + n \sum_i \langle \mathbf{R}_i^1 \nabla_i U \rangle + \frac{1}{2} n^2 \langle \mathbf{r} \nabla V \rangle \quad (1)$$

where \mathbf{P}_0 is due to the solvent and to externally imposed isotropic pressure. The term in n will not be considered further here, being basically intramolecular in nature (6); we shall presume it to be small compared with the intermolecular term in n^2 . Thus we are in effect restricting our attention to a range of concentration for which

* This somewhat slippery term shall refer, first of all, to a concentration range for which the theories pertaining to infinite dilution (that is, absolutely no interactions between polymer molecules) are inadequate. The lower end of this range depends on solvent and polymer molecular weight M , and a precise numerical figure cannot be assigned to it; it is often of order 1% when $M \sim 10^6$. The upper end of this intermediate range is characterized by severe entanglements between polymers, such that segmental spatial distributions are appreciably distorted from Gaussian when flow occurs and intermolecular potentials may not be additive pairwise. This upper limit is also difficult to characterize with a number, but may be of order 10 to 20% and should be very sensitive to M .

$$\mathbf{P} - \mathbf{P}_0 = \frac{1}{2} n^2 \langle \mathbf{r} \nabla V \rangle \quad (2)$$

where \mathbf{r} is the vector between centers of two polymer molecules and $V(\mathbf{r})$ is the intermolecular potential between them (6). The brackets $\langle \rangle$ represent an average in pair space, taken with respect to the pair correlation function $g(\mathbf{r})$.

Following Kirkwood and co-workers (13), we perform a linear shear perturbation on $g(\mathbf{r})$ and thereby introduce its equilibrium limit $g_0(\mathbf{r})$ and the friction coefficient ξ . If g_0 is approximated as unity in this concentration range (7), Equation (2) can be displayed conveniently as

$$\mathbf{P} - \mathbf{P}_0 = - \left[\frac{1}{2} n^2 \int V d\mathbf{r} \right] \mathbf{I} + \gamma \left(\frac{C \xi n^2}{2kT} \right) \int (\mathbf{r} \nabla V) \frac{xz}{r^3} d\mathbf{r} \quad (3)$$

wherein we have postulated steady simple shear flow ($\dot{\gamma}$ = shear rate)

$$\mathbf{v} = (v_x, 0, 0) = (\dot{\gamma}z, 0, 0) \quad (4)$$

and recognize ξ as a measure of the effectiveness of the $g(\mathbf{r})$ perturbation.

Next, we represent the intermolecular potential in general by (7, 8)

$$V(\mathbf{r}) = A \int \nu(\mathbf{R}) \nu(\mathbf{r} + \mathbf{R}) d\mathbf{R} \quad (5)$$

where $\nu(\mathbf{R})$ measures the probability of finding a polymer segment at position \mathbf{R} relative to the center of the molecule to which it belongs. The parameter A can be evaluated at equilibrium (7), but shall remain unidentified at present. We desire that $\nu(\mathbf{R})$ should represent a shear-deformable molecule; our selection, discussed elsewhere (26), is

$$\nu(X, Y, Z) = N \exp \{ -B [(X - mZ)^2 + (1 + m^2)(Y^2 + Z^2)] / (1 + m^2) \} \quad (6)$$

$$N = (B/\pi)^{3/2} / \sqrt{1 + m^2} \quad (7)$$

$$m = \lambda\dot{\gamma} \quad (8)$$

where λ is a time constant and N has been chosen to normalize the segment probability density $\int \nu(\mathbf{R}) d\mathbf{R} = 1$.

When Equations (6) and (7) are substituted into Equation (5), the result is

$$V = \frac{A}{\sqrt{1+m^2}} \left(\frac{B}{2\pi} \right)^{3/2} \exp \left\{ -B \left[(x-mz)^2 + (1+m^2)y^2 + (1+3m^2)z^2 \right] / 2(1+m^2) \right\} \quad (9)$$

STRESS PREDICTION

Examination of Equation (3) reveals that when $\gamma = 0$ (that is, at equilibrium) the stress tensor is isotropic:

$$\mathbf{P}_{eq} - p_o \mathbf{I} = \left[-\frac{1}{2} n^2 \int V(r) dr \right] \mathbf{I} \quad (10)$$

This becomes, with the introduction of Equation (9) evaluated at $m = 0$

$$\mathbf{P}_{eq} - p_o \mathbf{I} = -\frac{1}{2} n^2 A \mathbf{I} \quad (11)$$

and we see that A is (within the scope of this model) simply related to the osmotic pressure, an equilibrium thermodynamic property quite amenable to experimental evaluation. Because of our prior use of the simplification $g_o = 1$, Equation (11) contains only the energy parameter A . The parameter B , introduced in Equation (6) as a scale factor reflecting chain size, would appear in Equation (11) if better approximations to $g_o(r)$ were used.

Even when shear is present, \mathbf{P} in Equation (3) will have equal diagonal components (normal stresses) if V happens to be a symmetric potential. Thus if $\nu(\mathbf{R})$ were chosen to represent spherical and undeformable molecules, no normal stress differences would result [and a purely Newtonian viscosity would appear (13)]. In the present case, however, $\nu(\mathbf{R})$ in Equation (6) describes a molecular domain which is deformed anisotropically by the shearing forces. Substitution of Equation (9) into Equation (3) yields the normal components

$$P_{ii} - p_o = -\frac{1}{2} n^2 A \left(\frac{1+m^2}{1+3m^2} \right)^{1/2} \quad (i = x, y, z) \\ - \left(\frac{B}{2} \right)^{5/2} \frac{n^2 A C \xi \gamma}{kT[\pi(1+m^2)]^{3/2}} \cdot \iiint L K_i dx dy dz \quad (12)$$

where

$$L = \frac{xz}{(x^2 + y^2 + z^2)^{5/2}} \exp \left\{ -B \left[(x-mz)^2 + (1+m^2)y^2 + (1+3m^2)z^2 \right] / 2(1+m^2) \right\} \quad (13)$$

$$K_x = x^2 - mxz \quad (14)$$

$$K_y = (1+m^2)y^2 \quad (15)$$

$$K_z = (1+4m^2)z^2 - mxz \quad (16)$$

Since p_o is not a rheological function and does not influence the flow behavior of an (assumed) incompressible fluid, we shall discard it by computing only the differences between normal stress components:

$$P_{ii} - P_{jj} = - \left(\frac{B}{2} \right)^{5/2} \frac{n^2 A C \xi \gamma}{kT[\pi(1+m^2)]^{3/2}} \cdot \iiint L(K_i - K_j) dx dy dz \quad (i, j = x, y, z) \quad (17)$$

The integrals in Equation (17) may be evaluated con-

veniently after a unitary transformation of variables which diagonalizes the quadratic form in the exponent of L [see reference 26 for details]. Results will be expressed in terms of reduced variables:

$$(\pi_{ii} - \pi_{jj})_r \equiv (\pi_{ii} - \pi_{jj}) \left[\frac{-4kT\lambda}{n^2 A C \xi} \left(\frac{2\pi}{B^3} \right)^{1/2} \right] \quad (18)$$

which are dimensionless. For purposes of later discussion we shall next replace the indices (x, y, z) by $(1, 3, 2)$ and write the two normal stress functions—and, for comparison, the shear stress (26)—in compact form as

$$(P_{11} - P_{33})_r = a \{-b_3 + c_3 + c_3 d(F - 2E) + e_3 dF\} \quad (19)$$

$$(P_{11} - P_{22})_r = 4a \{-b_2 + c_2 + c_2 d(F - 2E) + e_2 dF\} \quad (20)$$

$$(P_{12} - \eta_s \gamma)_r = \frac{a}{m} \{-b + c + cd(F - 2E) + edF\} \quad (21)$$

wherein

$$a = [3\sqrt{1+m^2}(1+4m^2)(1+3m^2)^2]^{-1} \quad (22)$$

$$d = [(1+m^2)(2m\sqrt{1+4m^2})^{-1}]^{1/2} \quad (23)$$

$$b_3 = 19 + 108m^2 + 137m^4 + 32m^6 \quad (24)$$

$$b_2 = 5 + 30m^2 + 43m^4 + 10m^6 \quad (25)$$

$$b = 3 + 10m^2 - 27m^4 - 90m^6 - 48m^8 \quad (26)$$

$$c_3 = (9 + 96m^2 + 307m^4 + 284m^6 + 32m^8) \cdot (m\sqrt{1+4m^2})^{-1} \quad (27)$$

$$c_2 = (3 + 8m^2 - 23m^4 - 44m^6)m(1+4m^2)^{-1/2} \quad (28)$$

$$c = (3 + 12m^2 + 13m^4 + 60m^6 + 96m^8)m \cdot (1+4m^2)^{-1/2} \quad (29)$$

$$e_3 = 13 + 60m^2 + 31m^4 - 16m^6 \quad (30)$$

$$e_2 = 5 + 30m^2 + 47m^4 + 22m^6 \quad (31)$$

$$e = 3 + 10m^2 - 23m^4 - 78m^6 - 48m^8 \quad (32)$$

In Equations (19) to (21) the functions $F = F(\Phi, \kappa)$ and $E = E(\Phi, \kappa)$ are incomplete elliptic integrals of the

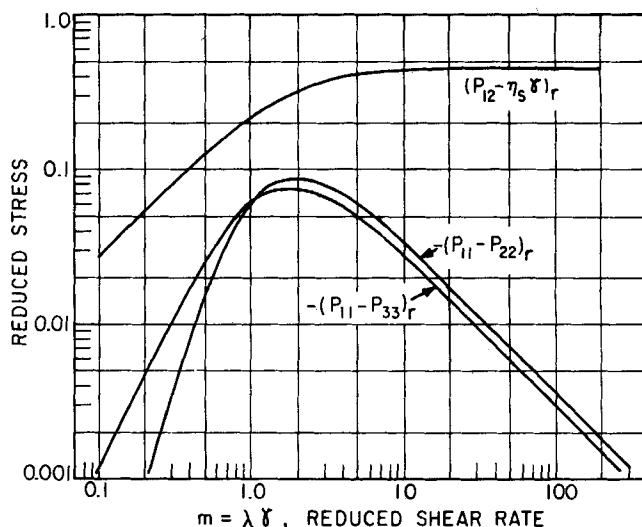


Fig. 1. Reduced dimensionless stresses from intermolecular forces alone, for simple shear flow $\gamma = dv_1/dx_2$. Stresses can be recovered by multiplying ordinates by $[-n^2 A C \xi B^{3/2} / 4 \sqrt{2\pi} kT\lambda]$. These curves correspond to Equations (19) to (21).

first and second kind (12):

$$\frac{E}{F} = \int_0^\Phi (1 - \kappa^2 \sin^2 \theta)^{\pm 1/2} d\theta \quad (33)$$

with

$$\kappa^2 = 0.5 + m^3 [(1 + m^2) \sqrt{1 + 4m^2}]^{-1} \quad (34)$$

$$\sin^2 \Phi = 2m [(1 + 2m^2) \sqrt{1 + 4m^2} - m(1 + 4m^2)] \cdot (1 + 3m^2)^{-1} \quad (35)$$

The shear rate parameter in Equations (22) to (36) is actually

$$m = \sqrt{\lambda^2 \gamma^2} \quad (8a)$$

which has appeared quite naturally as a mathematical consequence of the integrations, and is of course unaffected by a change of sign in γ . Equation (21) contains a/m where $m = \lambda\gamma$ as before, and hence the shear stress may change sign as γ does.

In Figure 1 is shown the shear-rate dependence of the stress functions, Equations (19) to (21). Asymptotic forms of some interest are displayed in Table 1.

DISCUSSION

Low Shear

The primary normal stress function ($P_{11} - P_{33}$) is seen from Figure 1 and Table 1 to be quadratic in shear rate in the lowest approximation, and in the same range the shear stress is linear in m . This is physically realistic and expected; most rheological models behave similarly. In this low-shear regime, we may compute the limiting (Newtonian) viscosity η_0 :

$$\eta_0 \equiv \frac{(P_{12})_0}{\gamma} = \frac{n^2 A \xi (-C) B^{3/2}}{15 \sqrt{2\pi} kT} + \eta_s \quad (36)$$

We may also express the limiting normal stress in terms of η_0 :

$$(P_{11} - P_{33})_0 = -\frac{3}{7} \lambda (\eta_0 - \eta_s) \gamma^2 \quad (37)$$

This illustrates explicitly how the normal stress is influenced by the time constant λ at low shear. Clearly a fluid with arbitrarily large η_0 might not exhibit measurable normal stresses if λ were small; that is, the fluid might appear inelastic.

The proportionality of $(P_{11} - P_{22})_0$ to m^4 is rather surprising and seems contrary to experience with viscoelastic materials. To order m^2 , the present model predicts $(P_{11})_0 \approx (P_{22})_0$, and in this limit agrees with the *inelastic* Reiner-Rivlin-Prager model for which $P_{11} = P_{22}$ at all shear rates. However, most measurements on elastic liquids (17, 22) indicate that $(P_{11} - P_{22})$ is nowhere near zero, but rather is comparable to $(P_{11} - P_{33})$ in magnitude. Measurements with a Weissenberg rheogoniometer,

which senses $(P_{11} - P_{22})$ directly, give no hint of stress approaching proportionality to γ^4 (9, 23). On the other hand, matters of instrument sensitivity and alignment—as well as polydispersity of sample—may explain this.

High Shear

In a preceding paper (26) it was pointed out that the prediction for $(P_{12} - \eta_s \gamma)$, based on the intermolecular contribution to shear stress, seemed inadequate by itself at high rates. It exhibited rather rapid saturation, approaching zero as $m \rightarrow \infty$, and hence $\eta_\infty \rightarrow \eta_s$. For real fluids, however, $\eta_\infty > \eta_s$. This failure of the model is due in part to inadequacies of $\nu(\mathbf{R})$ at high γ , and also to our total neglect of terms in c [see Equation (1)] which must ultimately become important even for concentrated solutions at high shear. For example, Merrill et al. (19) have found $(\eta_\infty - \eta_s) \sim c$ for several examples of such systems. Certainly the very presence of solute is sufficient to assure $\eta_\infty > \eta_s$.

The corresponding normal stress prediction is a rapid decrease ($\sim 1/m$) which has also never been observed directly. The usual behavior is a monotonic increase with γ , approaching near proportionality with m^1 at very high rates (18, 24). In one particular case, however, Adams and Lodge (1) reported that $(P_{11} - P_{22})$ as calculated from other measurements appeared to go through a maximum and then decrease markedly.

Still we must conclude that for most purposes the present model—incorporating only one time constant and many pseudolinear approximations—can have little utility at high rates. A physical explanation for some of its unrealistic predictions would be based on inadequacies of the segment distribution function $\nu(\mathbf{R})$. This function suggests correctly that a polymer molecule under high shear will become very elongated and oriented with a preferred axis approaching the streamline,* which would reduce the probability of molecules intermingling and flexing elastically. However, the ν used here is overly simple and thus exaggerates this behavior; one is thus forced ultimately to envision a fleet of very fine rigid needles aligned parallel to each other, moving along with minimal interaction. But in reality, the model used here for $\nu(\mathbf{R})$ would fail long before this extreme state were reached.

Intermediate Shear and Comparison with Data

For $m < 1$, the normal stress prediction displayed in Figure 1 seems to exhibit fairly realistic curvature; the shear stress curve might be useful to somewhat higher m . If the theory presented here and elsewhere (26) is valid,

* If ν in Equation (6) is used to calculate the moments $\bar{X}^2(m) = \int X^2 \nu(\mathbf{R}; m) d\mathbf{R}$, etc., we may compute gross shape ratios such as $(\bar{X}^2/\bar{Z}^2)^{1/2} = \sqrt{1 + 4m^2}$. This indicates a spherically symmetric molecule at zero shear, but an unrealistically elongated one at very high shear.

TABLE 1. ASYMPTOTIC FORMS OF REDUCED STRESS FUNCTIONS

Reduced shear rate limit	$(P_{11} - P_{33})_r$	$(P_{11} - P_{22})_r$	$(P_{12} - \eta_s \gamma)_r$
$m \rightarrow 0$	$-\frac{4}{35} \left(1 + \frac{25}{44} m^2 \right) m^2$	$-\frac{32}{63} m^4$	$\frac{4}{15} \left(1 - \frac{9}{14} m^2 \right) m$
$m \rightarrow \infty$	$-\frac{4}{27} \left(\frac{1}{m} \right)$	$-\frac{5}{27} \left(\frac{1}{m} \right)$	$\frac{4}{9}$

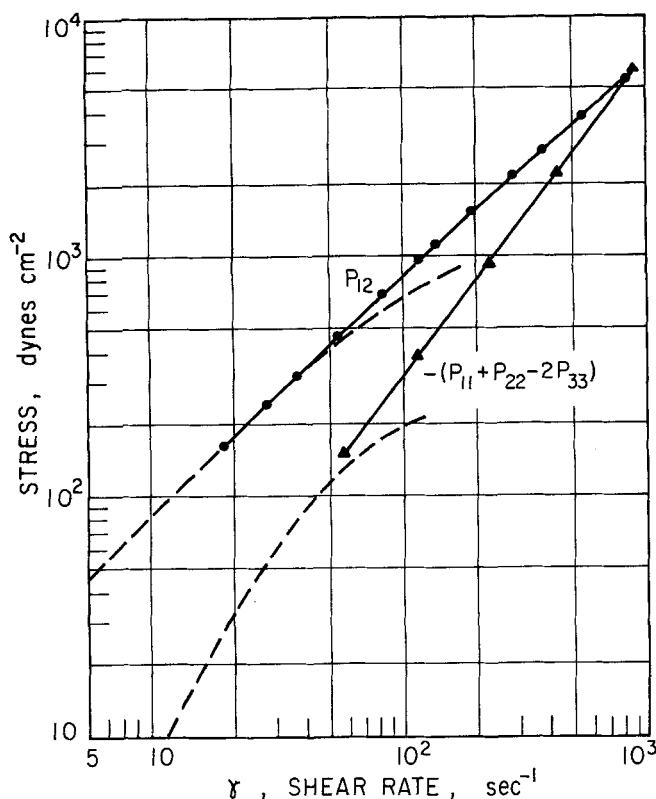


Fig. 2. Shear stress (●) and normal stress (▲) data for 8.0% polyvinyl alcohol in water (22). Solid curves, drawn by eye, represent the data. Dashed curves, similar to those shown in Figure 1, are the theoretical predictions with $\lambda = 0.012$ sec.

it must be able to represent *simultaneously* the normal and shear stress data on concentrated polymer solutions, at low shear.

Two tests of this are presented in Figures 2 and 3. Both plots contain data obtained in cone-and-plate instruments, and in both cases the data have been published elsewhere. The normal stress function appropriate to the cone-and-plate, calculated from the slope of the radial pressure profile, is $(P_{11} + P_{22} - 2P_{33})$. From Figure 1 we may extract this function as predicted by our theory. For example, at low shear

$$(P_{11} - P_{33})_0 + (P_{22} - P_{33})_0 = -\frac{6}{7}\lambda(\eta_0 - \eta_s)\gamma^2 \dots \quad (38)$$

The procedure for curve fitting is easy and the best fit unambiguous. Given the theoretical dimensionless curves for P_{12} and $(P_{11} + P_{22} - 2P_{33})$ on one graph, and the corresponding experimental curves on another, we adjust the relative positions of the coordinate axes of the two graphs until superposition is achieved. Whereas such a technique can be somewhat arbitrary when applied to one curve along (for example, P_{12}), it comes close to securing a unique fit when two types of curves are superimposed simultaneously as is done here.

Figure 2 shows the behavior of an 8.0% solution of polyvinyl alcohol (DuPont, Elvanol 72-51) in water (24), and Figure 3 represents a 6.86% solution of polyisobutylene (Badische Anilin, Oppanol B100) in cetane (16, 17). Neither polymer is monodisperse, which means that the entire range of liquid response cannot possibly be characterized by one distinct λ . Hence the exact curvature of the experimental data is perhaps less important than the relative magnitudes of P_{12} and $(P_{11} + P_{22} - 2P_{33})$ at low shear, which is always determined principally by the longest relaxation time.

Both Figures 2 and 3 demonstrate the quantitative inadequacies of the model. In both cases the experimental data just barely overlap the shear-rate region for which the model is hoped to be useful. Once the theoretical and experimental curves have been superimposed as closely as possible, λ may be evaluated easily from the numerical equality of the abscissas:

$$(\lambda\gamma)_{\text{theory}} = \gamma_{\text{data}} \quad (39)$$

A quick check on λ obtained in this fashion is obtained by rewriting Equation (38) to give

$$\lambda = -\frac{7}{6} \frac{(P_{11} + P_{22} - 2P_{33})_0}{(\gamma P_{12})_0} \quad (40)$$

(nearly so if $\eta_0 \gg \eta_s$). This, of course, may in principle be evaluated from the data directly, without recourse to a curve fitting procedure at all. We note, however, that frequently this low-shear stress limit is not experimentally accessible (see Figure 2), and extrapolations to low shear without a guiding model would be hazardous and subjective. For the data in Figure 2, we find $\lambda = 0.012$ sec. and from Figure 3, $\lambda = 0.25$ sec. These results are in agreement with both Equations (39) and (40).

Weissenberg Hypothesis

Since the two theoretical normal stress curves in Figure 1 are unequal, we see that $P_{22} \neq P_{33}$ and hence that the present model does not conform in general to the behavior of the hypothetical Weissenberg fluid ($P_{22} = P_{33}$). Instead, P_{22} and P_{33} are predicted to differ at low shear and to approach equality with increasing shear (near $m \approx 1$). In this respect, they appear to correspond to the observations of Ginn and Metzner (9). However, most reports of $(P_{22} - P_{33})$ indicate that its magnitude is a nearly fixed fraction of other normal stress functions (1, 10, 11, 17, 22, 25). These measurements, of course, are mostly conducted at shear rates so high that the present model is not expected to be too useful.

The full behavior of $(P_{22} - P_{33})$ is shown in Figure 4. We find that for $m < 1$, $(P_{22} - P_{33})$ has the *same sign*

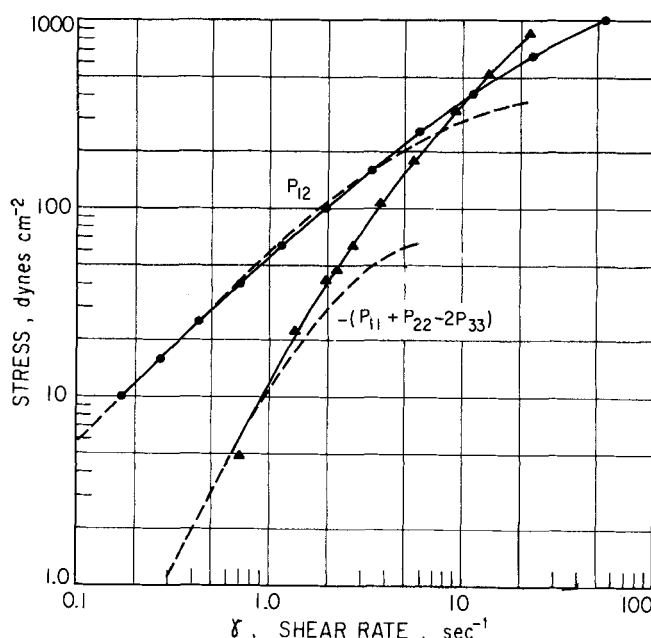


Fig. 3. Similar to Figure 2, for 6.86% polyisobutylene in cetane (15, 16). $\lambda = 0.25$ sec.

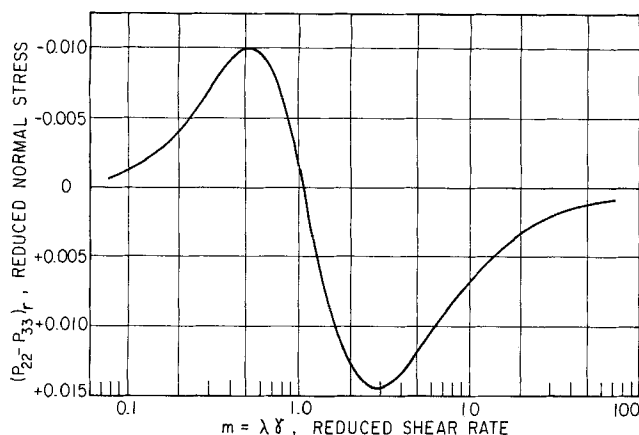


Fig. 4. Dimensionless secondary normal stress, obtained by subtracting the two normal stress curves in Figure 1.

as do $(P_{11} - P_{22})$ and $(P_{11} - P_{33})$ and likewise represents a tension. In this respect it agrees with most experimental results (10, 15, 17, 22) and represents an important improvement over other molecular theories which insist that the sign of $(P_{22} - P_{33})$ differs from those of the others (14, 20, 28).

When $m > 1$, we have the unexpected prediction that $(P_{22} - P_{33})$ changes sign and becomes, in effect, a net compressive stress. Such a change in sign has never been observed directly, but cannot be excluded from the realm of possible phenomena. In the case cited before, Adams and Lodge (1) pointed out that $(P_{11} - P_{22})$ obtained indirectly appeared to change sign at high shear. Furthermore, Jackson and Kaye (11) have recently reported measurements in a pseudo cone-and-plate geometry which indicate that $(P_{22} - P_{33})$ and $(P_{11} - P_{22})$ may have opposite signs. In the context of this discussion, we might look upon all these results collectively as limited evidence that normal stress functions can indeed change sign for some fluids, perhaps together and perhaps separately, and that the signs which are reported may depend on the shear-rate range of a particular investigation and the relative importance of intramolecular and intermolecular forces. We hasten to point out that the rapid change of $(P_{22} - P_{33})$ predicted in this work is a consequence of using an oversimplified $\nu(\mathbf{R})$ and ignoring intramolecular contributions to the stress. The function $(P_{22} - P_{33})$ is expected to be particularly sensitive to these approximations.

Concentration and Molecular Weight Dependence

For dilute solutions, many types of stress data may be correlated in terms of reduced variables which contain the first power of $c = nM/N$ (5). This is adequately explained by existing theory (5, 29), and indeed would arise from a consideration of the middle term of Equation (1) alone. In concentrated solutions the factor c^2 has proved more useful (4, 17, 24), or even c^3 (17). This was explained on the basis of the present model in another work (27) with regard to the shear stress and viscosity. Specifically, it was argued that

$$\lambda(M, c) \sim \frac{(\eta_0 - \eta_s)}{c^2 F(c)} \quad (41)$$

where $F(c)$ is a thermodynamic mixing parameter which in certain concentration ranges might be only weakly dependent on c . From this it followed directly that η/η_0 , as a function only of a reduced shear rate $m = \lambda\gamma$, should be correlated in terms of

$$m \sim \left[\frac{\eta_0 - \eta_s}{c^2 F(c)} \right] \gamma \quad (42)$$

as the independent parameter.

In a similar fashion, we may explain the reduction of normal stress data by extending Equation (38):

$$(P_{11} + P_{22} - 2P_{33}) = -\frac{6}{7} \left(\frac{\eta_0 - \eta_s}{\lambda} \right) \cdot (\lambda\gamma)^2 \cdot [1 + H(\lambda\gamma)] \quad (43)$$

Hence, multiplying by $\lambda/(\eta_0 - \eta_s)$, we have another reduced function which depends only on m . Introduction of Equation (41) leads to the stress variable which was deduced from successful correlations:

$$\frac{(P_{11} + P_{22} - 2P_{33})}{c^2 F(c)} \quad (44)$$

in which $c^2 F(c)$ might approach c^3 for very high concentrations.

It is important to note that the c^2 dependence displayed in Equations (41), (42), and (44) is a consequence solely of a consideration of intermolecular forces. When such forces are important, as they will be in even moderately concentrated solutions, the factor c^2 (or even a higher dependence) will be necessary. This is so even in the absence of physical entanglements between molecules or the existence of gelatinous structures in the fluid. Hence the dilute solution result (5, 29)

$$\lambda_{\text{dil}}(M, c) \sim \frac{(\eta_0 - \eta_s)M}{c} \quad (45)$$

arising from analyses which neglect such interaction, will clearly be inadequate.

The molecular weight dependence of normal stress can be extracted from Equations (38) and (41) by combining them:

$$\frac{1}{\gamma^2} (P_{11} + P_{22} - 2P_{33})_0 \sim \lambda(M) \cdot [\eta_0(M) - \eta_s] \sim [\eta_0 - \eta_s]^2 \sim \eta_0^2(M) \quad (46)$$

This result, too, differs from the dilute solution prediction which would be made with Equation (45):

$$\frac{1}{\gamma^2} (P_{11} + P_{22} - 2P_{33})_0|_{\text{dil}} \sim \lambda \cdot [\eta_0 - \eta_s] \sim M[\eta_0 - \eta_s]^2 \sim M[\eta]^2 \quad (47)$$

where $[\eta]$ is the intrinsic viscosity. Equations (46) and (47) are both independent of many details of a model, for either dilute or concentrated solutions. These details would be needed to evaluate $\eta_0(M)$ or $[\eta]$. For the dilute case (5, 8) $[\eta]$ can depend on molecular weight as $M^{0.5}$ to near M^1 for various solvents, and hence $(P_{11} + P_{22} - 2P_{33})_0 \sim M^2$ to M^3 from Equation (47). For the case of higher concentration, the present model has been used (27) to estimate $\eta_0 \sim M^{1.25}$ in the absence of entanglement effects. From Equation (46) this would give $(P_{11} + P_{22} - 2P_{33})_0 \sim M^{2.5}$, which is not markedly different from dilute solution results and seems much too weak. The latter remark may be unfair, since normal stresses are almost always measured for solutions wherein strong entanglement effects are likely, and thus we cannot state with certainty the experimentally determined M dependence for solutions which are relatively free of such effects (as assumed by the development here). If we use the experimental result (valid at high M , when entanglements exist) that $\eta_0 \sim M^{3.4}$, then Equation (46) indicates that $(P_{11} + P_{22} - 2P_{33})_0 \sim M^{6.8}$. This of course is not a strictly legitimate application of the present model but appears to agree better with some observations. A dependence of $M^{7.8}$ has also been suggested, based on the dilute solution result of Equation (47): $\lambda(\eta_0 - \eta_s) \sim \lambda\eta_0 \sim M\eta_0^2$.

Experimental data at the present time do not appear adequate to test these predictions. However, the possibility that normal stress varies approximately as M^7 for some materials is not surprising to those who have performed experiments. It helps to explain why many early investigators, working with polymers of modest size ($M \sim 10^4$), did not report anomalous Weissenberg phenomena. Clearly these effects are unmistakable when $M \sim 10^6$.

CONCLUSIONS

A consideration of intermolecular forces in concentrated polymer solutions has led to the prediction of non-Newtonian viscosity and two normal stress functions for the shear flow, $v_1 = \gamma x_2$. Only two phenomenological parameters are required, a low-shear limiting viscosity η_0 and a time constant λ . The predicted shear dependency of the stresses is realistic up to moderate shear rates ($\lambda\gamma \approx 1$). Within this range ($P_{11} - P_{33}$) and ($P_{22} - P_{33}$) are predicted to have the same sign, a result in agreement with most experiments but not predicted by many other theories. For higher shear rates, stress behavior of this model becomes inadequate to approximate that of real fluids; in this regard, the present development cannot compete with many clever empirical models based on continuum mechanics (2, 23). This deficiency might be remedied by the introduction of higher order time constants and simultaneous consideration of intramolecular effects. We have not yet explored the ability of this model to describe time-dependent phenomena (for example, to predict the complex viscosity η^* measured in sinusoidal shear); it seems to be possible, although nontrivial.

The experimentally established utility of the factor c^2 on both coordinates in master plots of normal stress data for concentrated solutions can be justified with the present model. Predictions about molecular weight effects are not expected to be valid at extremely high M (when entanglements are important), but await testing.

ACKNOWLEDGMENT

Acknowledgment is made to the donors of the Petroleum Research Fund, administered by the American Chemical Society, for support of this research.

NOTATION

- a = dimensionless coefficient, function of shear rate, used to describe non-Newtonian stress behavior, Equation (22)
- A = constant determining magnitude of intermolecular potential, Equation (5), and related to osmotic pressure, Equation (11); (g.) (cm.⁵)/sec.²
- b, b_2, b_3 = dimensionless coefficients, Equations (24) to (26); see a
- B = stiffness parameter characterizing a pseudo Gaussian segment distribution, Equation (6), cm.⁻²
- c = mass concentration, g./cc.
- c, c_2, c_3 = dimensionless coefficients, Equations (27) to (29); see a
- C = integration constant which specifies strength of the shear perturbation of $g_0(r)$, cm.⁵
- d = dimensionless coefficient, Equation (23); see a
- e, e_2, e_3 = dimensionless coefficients, Equations (30) to (32); see a
- E, F = incomplete elliptic integrals of the second and first kinds, Equation (33)
- $F(c)$ = dimensionless concentration-dependent parameter, related to A
- $g(r), g_0(r)$ = pair correlation function and its equilibrium limit (radial distribution function), dimensionless
- \mathcal{H} = dimensionless function of shear rate, Equation (43)

- I = unit tensor
- k = Boltzmann's constant, 1.38×10^{-16} , (g.) (sq. cm.)/(sec.²) (deg.)
- K_i = part of integrand in Equation (12), see Equations (14) to (16); sq. cm.
- L = part of integrand in Equation (12), see Equation (13); cc.⁻¹
- m = $\gamma\lambda$, dimensionless shear rate
- M = molecular weight of a flexible polymer, g./mole
- n = number density of polymer molecules, cc.⁻¹
- N = number of statistical segments in each polymer molecule
- N = Avogadro number
- \mathcal{N} = normalizing coefficient for $\nu(\mathbf{R})$, Equation (7)
- p_0 = isotropic pressure contribution which would exist in the absence of polymer solute, g./ (cm.) (sec.²)
- P, P_{ij}, \mathbf{P}_0 = total stress tensor, its ij component, and that portion of it which would exist in the absence of polymer solute, g./ (cm.) (sec.²)
- \mathbf{r} = vector separation of centers of two polymer molecules, cm.
- \mathbf{R} = vector position, referred to the center of a polymer molecule, cm.
- T = absolute temperature
- U = potential of mean force due to the presence of all segments, (g.) (sq. cm.)/sec.²
- \mathbf{v}, v_i = velocity vector and its i^{th} component, cm./sec.
- $V(r)$ = intermolecular potential energy, derivable from U (5), (g.) (sq. cm.)/sec.²
- x, y, z = components of \mathbf{r} , cm.
- X, Y, Z = components of \mathbf{R} , cm.

Greek Letters

- γ = dv_1/dx_2 , shear rate in simple shear flow, sec.⁻¹
- $\eta(m), \eta_0, \eta_\infty$ = non-Newtonian viscosity, its low-shear limit, and its high-shear limit; g./ (cm.) (sec.)
- $[\eta]$ = intrinsic viscosity, $\lim c \rightarrow 0 [(\eta_0 - \eta_s)/c\eta_s]$, cc./g.
- η_s = solvent viscosity, g./ (cm.) (sec.)
- θ = polar coordinate, rad.
- κ = parameter of elliptic integrals, Equation (34); dimensionless
- λ = time constant for polymer chain response, sec.
- $\nu(\mathbf{R})$ = probability density for distribution of polymer segments about their own molecule, cc.⁻¹
- ξ = friction coefficient between polymer molecules, g./sec.
- Φ = amplitude of elliptic integrals, Equation (35), rad.

LITERATURE CITED

1. Adams, N., and A. S. Lodge, *Phil. Trans. Roy. Soc. (London)*, **A256**, 149 (1964).
2. Bogue, D. C., *Ind. Eng. Chem. Fundamentals*, **5**, 253 (1963); with J. O. Doughty, p. 243.
3. Bueche, F., *J. Chem. Phys.*, **20**, 1959 (1952).
4. DeWitt, T. W., H. Markovitz, F. J. Padden, and L. J. Zapas, *J. Colloid Sci.*, **10**, 174 (1955).
5. Ferry, J. D., "Viscoelastic Properties of Polymers," Wiley, New York (1961).
6. Fixman, M., *J. Chem. Phys.*, **42**, 3831 (1965).
7. *Ibid.*, **35**, 889 (1961).
8. Flory, P. J., "Principles of Polymer Chemistry," Chap. 10, 12, Cornell Univ. Press, Ithaca, N. Y. (1953).
9. Ginn, R. F., and A. B. Metzner, in "Proc. 4th Intern. Cong. Rheology," Vol. 2, p. 583, Interscience, New York (1965).
10. Huppler, J. D., *Trans. Soc. Rheol.*, **9B**, 273 (1964).
11. Jackson, R., and A. Kaye, *Brit. J. Appl. Phys.*, **17**, 1355 (1966).
12. Jahnke, J. H., and F. Emde, "Tables of Functions," 4 ed., Dover, New York (1945); for F and E to seven significant figures, see V. M. Belyakov, P. I. Kravtsova,

- and M. G. Rappoport, "Tables of Elliptic Integrals," Pt. I, Pergamon, New York (1965).
13. Kirkwood, J. G., F. P. Buff, and M. S. Green, *J. Chem. Phys.*, **17**, 988 (1949).
 14. Kotaka, T., *ibid.*, **30**, 1566 (1959).
 15. Lodge, A. S., "Elastic Liquids," Academic Press, New York (1964); *Trans. Faraday Soc.*, **52**, 120 (1956).
 16. Markovitz, H., private communication (Mar., 1966).
 17. ———, and D. Brown, *Trans. Soc. Rheol.*, **7**, 137 (1963).
 18. Markovitz, H., and B. Williamson, *ibid.*, **1**, 25 (1957).
 19. Merrill, E. W., H. S. Mickley, and A. Ram (with G. Perkinson), *ibid.*, **5**, 237 (1961); with W. H. Stockmayer, **6**, 119 (1962).
 20. Mooney, M., *J. Polymer Sci.*, **34**, 599 (1959).
 21. Rouse, P., *J. Chem. Phys.*, **21**, 1272 (1953).
 22. Sakiadis, B. C., *AIChE J.*, **8**, 317 (1962).
 23. Spriggs, T. W., J. D. Huppler, and R. B. Bird, *Trans. Soc. Rheol.*, **10**, No. 1, 191 (1966).
 24. Williams, M. C., *AIChE J.*, **11**, 467 (1965).
 25. ———, *Chem. Eng. Sci.*, **20**, 693 (1965).
 26. ———, *AIChE J.*, **12**, 1064 (1966).
 27. *Ibid.*, **13**, 534 (1967).
 28. Yamamoto, M., *J. Phys. Soc. Japan* **11**, 413 (1956); **12**, 1148 (1958); **13**, 1200 (1958).
 29. Zimm, B. H., *J. Chem. Phys.*, **24**, 269 (1956).

Manuscript received November 22, 1966; revision received January 23, 1967; paper accepted January 25, 1967.

Transient Multicomponent Diffusion with Heterogeneous Reaction

J. L. HUDSON

University of Illinois, Urbana, Illinois

The problem of transient multicomponent diffusion of an arbitrary number of components in one-dimension with heterogeneous reaction has been solved exactly by means of the Laplace transform. Linearized expressions for the diffusion and reaction were used. Numerical evaluations of the solution are given and a comparison made with results derived by use of an effective diffusivity.

The momentum and continuity equations for multicomponent mass transfer with chemical reaction in an isothermal system are coupled and nonlinear. These equations can be simplified considerably if the concentration variations throughout the system are small, if the concentrations are not too far from chemical equilibrium, and if there is no volume change with reaction or mixing. Under these conditions the flux of any component can be expressed as a linear combination of the concentration gradients of each species (2, 5 to 9), the reaction rate expressions can be linearized (10), and the momentum equation can be solved independently of the continuity equations for each species (6). The problem thus reduces to solving a set of coupled, linear differential equations representing continuity of each component. The approximations involved in a linearization of the transport equations (6 to 8) and of the reaction rate expressions (10) have been clearly discussed in detail elsewhere.

When no chemical reaction is taking place, and when the concentration or flux of each component is known on the boundaries, the problem may be resolved by a rotation of the coordinate axes, which uncouples the continuity equations (6 to 8). If the equations are doubly coupled, this rotation will not in general uncouple the set. This double coupling may occur in the volume, as by diffusion

and homogeneous reaction, or in the volume and on the boundaries, as by diffusion and either heterogeneous reaction or transport between two phases. It would be fortuitous if one rotation would uncouple such a system, and this occurs only in very special circumstances as pointed out by Toor (9).

In general, systems which exhibit dual coupling will have to be treated numerically or approximately. However, in some special geometries transient coupled problems can be solved exactly, and these solutions will lead to an understanding of the characteristics of more complicated problems. Toor has obtained an exact solution to the problem of transient multicomponent diffusion with homogeneous chemical reaction in a finite one-dimensional region (9). In this work, transient multicomponent diffusion with heterogeneous reaction will be reported. The geometry chosen was the simplest possible, namely, a stagnant film.

ANALYSIS

Consider multicomponent diffusion of $N + 1$ components through a film with heterogeneous reaction taking place. The system is initially at steady state with a mole fraction distribution (f), where the components of (f) are